月旦知識庫

Garambullo (*Myrtillocactus geometrizans*) reduces cell viability via apoptosis and inhibits colony formation in HT-29 and SW480 colon cancer cell lines

López-Alvarez Guadalupe Soledad [a], Gutierrez-Silerio Gloria Yareli [a], García-Solís Pablo [a], Morales-Bárcenas Rocio [b], Sánchez-Pérez Yesennia [b], Hernández-Puga Ana Gabriela [a], Vergara-Castañeda Haydé Azeneth [a,*]

[a] Center for Advanced Biomedical Research, Faculty of Medicine, Autonomous University of Queretaro, Santiago de Querétaro 76140, Mexico
[b] Subdirección de Investigación Básica, Instituto Nacional de Cancerología, Mexico City, 14080, Mexico

Abstract

Garambullo (*Myrtillocactus geometrizans*) is a Mexican wild fruit rich in phytochemicals. In this study, freeze-dried garambullo was subjected to *in vitro* gastrointestinal digestion and fermentation. The resulting fermented extract of garambullo (FEG) was evaluated for its effects on cell viability in HT-29 and SW480 CRC cell lines using MTT assays. After 24 h of treatment, FEG exhibited IC_{50} values of 2985 μg/mL and 3200 μg/mL in HT-29 and SW480 cells, respectively, indicating a significant reduction in cell viability compared to the control group. This reduction was further confirmed by flow cytometry, which revealed increased late apoptosis and necrosis in HT-29 cells, and a pronounced increase of necrosis in SW480 cells treated with FEG. Molecular docking simulations further supported these findings, demonstrating that butyric acid, a metabolite identified in FEG, demonstrates energetically favorable interactions with Caspase-3 (Δ*G*: −5.41 kcal/mol) and RIPK1 (Δ*G*: −5.18 kcal/mol), suggesting potential multi-pathway involvement in apoptotic and necrosis-associated cell death. Furthermore, the colony-forming ability of these CRC cell lines was assessed using 3D culture assays. After 14 days, FEG reduced colony formation in SW480 cells, with complete suppression observed at 149 μg/mL. Notably, HT-29 cells exhibited greater sensitivity, as no colonies were detected at any of the tested concentrations (≥37 μg/mL). These findings indicate that FEG exerts significant anti-proliferative, pro-apoptotic, and anti-clonogenic effects in CRC cell lines, supporting its potential as a candidate for further investigation in therapeutic or preventive strategies.

Keywords: Butyric acid, Colorectal cancer, Garambullo, Molecular docking, Programmed cell death

1. Introduction

Myrtillocactus geometrizans is a member of the cactus family and an endemic species to the arid and semi-arid regions of Mexico. Its wild fruit, commonly known as garambullo, is an edible berry characterized by its spherical shape, with an average diameter of 1.5 cm and a height of 1.2 cm, and a deep purple color when fully ripe [1,2]. A bioactive profile of garambullo has been reported to include 43 different metabolites, notably 8 betaxanthins, 8 betacyanins, 13 flavonoids, and 6 phenolic acids, all of which contribute to its antioxidant capacity [2,3]. Several of these metabolites were also identified in a recent study conducted by our research group, using an *in vitro* gastrointestinal digestion model, a valuable method for assessing the nutraceutical bioavailability of phytochemicals in fruits such as garambullo [4]. In recent years, scientific interest in berries has increased due to their high content of phytochemicals, a class of plant-derived bioactive compounds with diverse chemical structures, particularly polyphenols such as anthocyanins, flavonols, tannins, phenolic acids,

Received 19 November 2025; accepted 17 April 2026.
Available online 30 July 2026

* Corresponding author.
E-mail address: hayde.vergara@uaq.mx (V.-C. Haydé Azeneth).

https://doi.org/10.38212/2224-6614.3599
2224-6614/© 2026 Taiwan Food and Drug Administration. This is an open access article under the CC-BY-NC-ND license (http://creativecommons.org/licenses/by-nc-nd/4.0/).

月日知識庫

stilbenes, and lignans [5]. These compounds have been associated with a range of biological activities, including antioxidants, anti-inflammatory, antimicrobial, antihyperglycemic, and anticancer effects [5,6]. In this context, *in vitro* gastrointestinal digestion models have emerged as a well-established tool for evaluating the bioavailability and potential biological activity of berry-derived phytochemicals. These models allow simulation of physiological conditions, enabling identification of metabolite transformations that may enhance or diminish their antiproliferative activity [7].

Indeed, several studies have demonstrated antiproliferative effects of digested berry extracts in colon cancer cell lines. For example, juice from Andean berry (Vaccinium meridionale) showed dose-dependent cytotoxicity in SW480 cells [7], while extracts from Arctic bramble, cloudberry, lingonberry, and strawberry inhibited proliferation of CaCo-2 cells with EC_{50} values ranging from 22.2 to 38.3 μg/mL [8]. Similarly, anthocyanin-rich extracts (AREs) from chokeberry significantly reduced viability in HT-29 cells, achieving 50% inhibition at 25 μg/mL after 48 h [9]. Complementary *in vivo* studies have further demonstrated the chemopreventive effects of AREs. In male Fischer 344 rats treated with azoxymethane, extracts from bilberry, chokeberry, and grape significantly reduced the formation of aberrant crypt foci and downregulated COX-2 expression, suggesting their potential role in colon cancer prevention [10]. The bioactive profile of garambullo is particularly relevant in this context, as it contains higher levels of betalains, phenolic compounds, and anthocyanins than many commonly studied berries [6]. Recent advances in the microencapsulation of garambullo extracts have focused on preserving their bioactivity and improving stability during gastrointestinal digestion and storage [6]. Importantly, its phenolic compounds and betalains are bioaccessible and stable after simulated gastrointestinal digestion, meaning they can potentially reach the colon and exert biological effects [6]. Thus, employing a human digestion model provides a more physiologically relevant assessment of garambullo's antiproliferative potential on CRC cells [7,10].

Diets rich in fruits, vegetables, nuts, and whole grains provide a wide array of phytochemicals that have demonstrated various health-promoting effects [11,12]. Moreover, poor dietary habits, such as the consumption of red and processed meats, are considered key risk factors for CRC, while phytochemical-rich diets are associated with reduced risk [13,14]. During colonic fermentation, these phytochemicals and non-digestible carbohydrates are metabolized by microbiota, leading to the production of short-chain fatty acids (SCFAs) and other bioactive metabolites. Notably, in a previous study from our group, metabolomic profiling of garambullo subjected to *in vitro* fermentation identified butyric acid as one of the SCFAs significantly increased after 24 h of fermentation. [15]. Given the well-documented role of short-chain fatty acids, particularly butyric acid, in modulating cell proliferation and apoptosis, these findings suggest a potential mechanistic link between fermented garambullo metabolites and colorectal cancer progression. During cancer development, or carcinogenesis, a series of progressive events occur, including genetic and epigenetic alterations, which collectively lead to tumorigenesis and metastasis. Among the distinctive hallmarks of carcinogenesis are sustained proliferative signaling and resistance to cell death [16,17], characteristics prominently observed in CRC [18]. In 2020, approximately 19.3 million new cancer cases were reported worldwide, resulting in an estimated 9.9 million cancer-related deaths. CRC ranks as the third most diagnosed cancer and the second leading cause of cancer-related mortality globally [19,20]. Considering this, there is increasing interest in identifying natural compounds with the potential to inhibit tumor progression.

In our recent *in vivo* study using male Sprague Dawley rats exposed to AOM/DSS, dietary administration of extractable and non-extractable phenols and betalains from garambullo (berry and residue) significantly reduced the formation of aberrant crypt foci and mitigated colonic epithelial injury after a two-week pretreatment period, suggesting a statistically significant chemopreventive effect during early stages of colon carcinogenesis [21]. This adds to the evidence supporting the relevance of garambullo-derived compounds in the prevention of CRC. In this context, peniocerol, a sterol isolated from garambullo, has been reported to inhibit cell growth and induce apoptosis *in vitro* in several CRC cell lines, including SW-620, HCT-15, and HCT-116 [22]. Other sterols from garambullo, such as macdougallin and peniocerol, have demonstrated antiproliferative effects, cell cycle arrest predominantly at the G0/G1 phase, and apoptosis in HCT-15 colon cancer cells [23].

The antitumoral properties of natural compounds, particularly their apoptotic and antiproliferative effects, have traditionally been studied using 2D monolayer cultures [24,25]. However, in the present study, we also investigated the effects of a fermented extract of garambullo (FEG) in a 3D cell culture model. Therefore, this study aimed, for the first time, to evaluate the effects of FEG, obtained

月日知識庫

through an *in vitro* simulation of gastrointestinal digestion and fermentation, on cell viability, apoptosis, and colony formation in HT-29 and SW480 CRC cell lines. Additionally, molecular docking was employed to provide a mechanistic rationale for the potential interactions between the previously identified butyric acid and key markers of programmed cell death.

2. Materials and methods

2.1. Fruit sample

Garambullo fruits were harvested in June 2020 from naturally growing *Myrtillocactus geometrizans* plants located in El Garabatillo, Dolores Hidalgo, Guanajuato, Mexico. The harvest was authorized by Ms. Josefina López Mata, a representative of local garambullo harvesters and processors, who granted permission for collection on her private property. The plant material used in this study corresponds to *Myrtillocactus geometrizans* (Mart. ex Pfeiff.) Console (family Cactaceae). A voucher specimen was deposited in the publicly accessible Herbarium of Querétaro "Dr. Jerzy Rzedowski" (QMEX), where the identification was formally confirmed by M.Sc. Yolanda Pantoja Hernández. The specimen is available for consultation under the accession number QMEX00007982.

Firm, purple-colored fruits were selected, washed with water, and subsequently freeze-dried using a Labconco Stoppering Tray Dryer (Model 7755013, Kansas City, MO, USA) at −40 °C, with a pressure of 0.133 mbar (13.3 Pa) maintained for 7 days. The resulting fruit powder was vacuum-sealed in airtight bags and stored at −80 °C.

2.2. In vitro *digestion*

The digestive process, including the oral, gastric, intestinal, and colonic fermentation phases, was simulated following a previously described protocol [26]. Four fasting volunteers, who had provided informed consent, had no history of gastrointestinal disorders, and followed an omnivorous diet, rinsed their mouths with water prior to chewing 1 g of freeze-dried garambullo for 15 s. The chewed material was then expectorated into a beaker. This procedure was repeated five times per participant. Between each chewing session, subjects rinsed their mouths with 5 mL of distilled water for 60 s, and the rinse was also collected in the same beaker. Additionally, a blank control was prepared by repeating the same procedure using only distilled water instead of garambullo. Both the garambullo sample and the blank were adjusted to pH 2.0 using 2N HCl. Subsequently, 0.055 g of pepsin (Sigma–Aldrich, 1003410749, USA), previously dissolved in 0.94 mL of 20 mM HCl, was added to each sample. Samples were then incubated at 37 °C in a water bath for 2 h to simulate gastric digestion [26]. For the intestinal phase, a simulated intestinal juice solution was freshly prepared 30 min prior to use by dissolving 3 mg of ox gall (Sigma–Aldrich, 8008-63-7, Germany) and 2.6 mg of pancreatin (Sigma–Aldrich, 232-468-9, Germany) in 5 mL of Krebs–Ringer buffer (composition: 118 mM NaCl, 4.7 mM KCl, 1.2 mM $MgSO_4$, 1.2 mM KH_2PO_4, 25 mM $NaHCO_3$, 11 mM glucose, and 2.5 mM $CaCl_2$; pH 6.8). A 5 mL aliquot of the intestinal juice was added to each digested sample and its corresponding blank [26]. The mixtures were then transferred into dialysis tubes (7 cm in length, sealed at both ends) and incubated at 37 °C for 30 min to simulate the intestinal absorption phase [27].

2.3. In vitro *fermentation*

In vitro fermentation of garambullo was carried out following the methodology described by Campos-Vega [26]. A basal medium was prepared with the following composition (g/L): casein peptone, 2 g; yeast extract, 2 g; NaCl, 1 g; K_2HPO_4, 0.04 g; KH_2PO_4, 0.04 g; $MgSO_4 \cdot 7H_2O$, 0.01 g; calcium chloride dihydrate, 0.01 g; $NaHCO_3$, 2 g; cysteine hydrochloride, 0.5 g; bile salts, 0.05 g; Tween-80, 2 mL. Additionally, 10 μL of vitamin K_1 (Sigma V3501-1G, Germany) and 0.05 g of hematin (previously weighed and dissolved in 5 mL of 1 M NaOH) were added. The final pH of the medium was adjusted to 7.0. Prior to fermentation, tubes designated for each treatment were filled with 9 mL of the basal medium, which had been previously gasified by bubbling a mixture of hydrogen, carbon dioxide, and nitrogen (10:10:80 v/v) for 30 min. The non-digestible fraction (NDF) obtained from the *in vitro* digestion process was centrifuged at 5000 rpm for 10 min to separate it into solid and liquid phases. For each fermentation tube, 100 mg of the solid phase, 100 μL of the liquid phase, and 1 mL of freshly prepared fecal solution were added and vortexed thoroughly. The fecal solution was prepared by homogenizing 1.5 g of fresh fecal samples from two healthy donors in 27 mL of phosphate-buffered saline (PBS). As a positive fermentation control, 100 mg of raffinose was used in place of the NDF phases. Additionally, 200 μL of a blank control (containing only water and saliva from the volunteers, without freeze-dried garambullo) was included. All tubes were then connected to a fermentation grid and incubated in a water bath at

月日知識庫

37 °C for 24 h. The resulting samples, referred to as fermented extract of garambullo (FEG), were protected from light and stored at −70 °C until further use in cell culture assays.

2.4. Cell viability assays

HT-29 and SW480 human colorectal adenocarcinoma cell lines were purchased from the American Type Culture Collection. Cells were seeded at a density of 1×10^4cells per well in 96-well plates containing 200 μL of complete culture medium per well. The medium consisted of Dulbecco's Modified Eagle Medium (DMEM; high glucose, Gibco 12-800-017) supplemented with 10% fetal bovine serum (FBS; Gibco 26140079, Qualified, USA) and 1% antibiotic-antimycotic solution (Gibco 15240062). Plates were incubated at 37 °C in a humidified atmosphere with 5% CO_2. After 24 h, the medium was replaced with fresh medium containing FEG at concentrations of 3468, 2973, 2478, 1982, and 1487 μg/mL. A control group without FEG was included, and all treatments were diluted in DMEM supplemented with 2% FBS and 1% antibiotic-antimycotic and incubated for 24 h. Following treatment, the media were removed, and 200 μL of MTT solution (Thiazolyl Blue Tetrazolium Bromide, Sigma M5655) at a final concentration of 0.5 mg/mL in 1X phosphate-buffered saline (PBS; Gibco 70011044) was added to each well. Plates were incubated for 1 h at 37 °C. After incubation, the MTT solution was carefully removed, and 200 μL of dimethyl sulfoxide (DMSO; Sigma–Aldrich 472301) was added to each well to dissolve the resulting formazan crystals. Plates were incubated for an additional 15 min. Absorbance was measured at 570 nm using a microplate reader (Varioskan Flash, Thermo Scientific). The average optical density (OD) of each treatment group was normalized to the untreated cells, which was set to 100% viability. Cells treated with 70% ethanol were used as a positive control for cytotoxicity and were considered 0% viability. IC_{50} values were calculated by interpolation of the dose–response data and were used as reference concentrations for flow cytometry analyses.

2.5. Apoptosis evaluation

HT-29 and SW480 CRC cells were seeded at a density of 7×10^5cells per well in 12-well plates containing DMEM supplemented with 10% FBS and 1% antibiotic-antimycotic solution. After 24 h of incubation, the culture medium was replaced with DMEM containing 2% FBS and treated with either 2985 μg/mL or 3200 μg/mL of FEG. These concentrations correspond to the IC_{50} values previously determined by MTT assay for HT-29 and SW480 cells, respectively. Cells were exposed to the indicated treatments for 4 and 24 h, and 5 mM hydrogen peroxide (H_2O_2) was used as a positive control for apoptosis. Following treatment, apoptosis was assessed using flow cytometry with the Annexin V-FLUOS Staining Kit (Roche, Ref. 11858777001), according to the manufacturer's instructions. Samples were analyzed using a BD FACSCanto II Clinical Flow Cytometry System. Data were processed using BD FACSDiva software, and apoptotic populations were expressed as percentages of total analyzed events. Statistical analyses were performed using GraphPad Prism 6 as described in the Statistical Analysis section.

2.6. Colony formation in agarose (3D assay)

Three-dimensional (3D) assays were conducted in 48-well plates using a two-layer agarose system. The bottom layer consisted of 0.6% agarose (Agarose E, Pronadisa 8100.10, Spain) in DMEM supplemented with 10% FBS, 1% antibiotic-antimycotic, and 0.1% DMSO. The middle layer consisted of 0.3% agarose in DMEM (same supplementation as the bottom layer) containing HT-29 or SW480 cells at a density of 5×10^4cells per well. Cells were treated with FEG at concentrations of 0 μg/mL, 37 μg/mL, 74 μg/mL, and 149 μg/mL. Both agarose layers were allowed to solidify for 20–30 min before adding a final surface layer of liquid DMEM containing the corresponding concentrations of FEG (0 μg/mL, 37 μg/mL, 74 μg/mL, and 149 μg/mL). Plates were incubated at 37 °C in a humidified atmosphere with 5% CO2. Fresh DMEM with or without FEG was added to the appropriate wells every three days. After 14 days, 0.5 mg/mL of nitrotetrazolium blue chloride (NBT; Invitrogen, 93862, USA) in PBS was added to each well, and the plates were incubated overnight under the same conditions. Subsequently, three representative fields per well were captured using a Luzeren microscope equipped with a camera and Velab software. The number of colonies was counted for each field, and the average was calculated for each treatment.

2.7. Molecular docking analysis

The binding affinity of butyric acid toward Caspase-3 (PDB: 3DEI) and RIPK1 (PDB: 4I5C) was evaluated using the SwissDock web server, based on the EADock DSS algorithm. Protein structures were retrieved from the Protein Data Bank, and the ligand was prepared using SwissParam. Docking was performed using the Accurate mode, and the

月日知識庫

most stable clusters were selected based on Full-Fitness and Gibbs free energy (ΔG) scores.

2.8. Statistical analysis

All experiments were performed in triplicate across two or three independent assays, and results are presented as mean ± SD. Data were analyzed using GraphPad Prism 6. Depending on the experimental design, statistical differences were evaluated by one-way ANOVA followed by Dunnett's multiple comparisons test (for comparisons versus untreated cells) or by two-way ANOVA followed by Tukey's post hoc test (for multiple group comparisons). In all cases, a p-value <0.05 was considered statistically significant. Statistical significance is indicated in the corresponding figure legends using either asterisks (*$p < 0.05$, **$p < 0.01$, ***$p < 0.001$, ****$p < 0.0001$) or different letters, as appropriate.

3. Results

3.1. FEG decreases cell viability in HT-29 and SW480 CRC cell lines

Following FEG treatment, both HT-29 and SW480 cells exhibited a marked decrease in cell density compared with untreated cells. Moreover, SW480 cells lost their characteristic elongated morphology, displaying a more rounded and detached appearance. These morphological alterations suggest a cytotoxic effect of FEG on colorectal cancer cells. Representative micrographs illustrating these changes are shown in Fig. 1A–D. Cell viability was evaluated by MTT assay in HT-29 and SW480 colorectal cancer cell lines treated with FEG concentrations ranging from 1487 μg/mL to 3468 μg/mL. In HT-29 cells, an IC_{50} value of 2985 μg/mL was determined. A statistically significant reduction in cell viability was observed only at 2973 μg/mL ($p < 0.001$) and 3468 μg/mL ($p < 0.01$) FEG compared to untreated cells (Fig. 1E). The strongest reduction in viability occurred at 3468 μg/mL and 2973 μg/mL FEG, resulting in 41.1% and 50.7% viability, respectively, compared with untreated cells. In contrast, concentrations of 2478 μg/mL and 1982 μg/mL FEG showed no inhibitory effect, with viability values above 100% (103% and 113%, respectively) at 24 h post-treatment (Fig. 1E). In SW480 cells, an IC_{50} of 3200 μg/mL was obtained (Fig. 1E). A statistically significant reduction in cell viability was observed at 1982 μg/mL ($p < 0.01$), 2478 μg/mL ($p < 0.05$), 2973 μg/mL ($p < 0.001$), and 3468 μg/mL ($p < 0.0001$) FEG compared to untreated cells. Treatment with

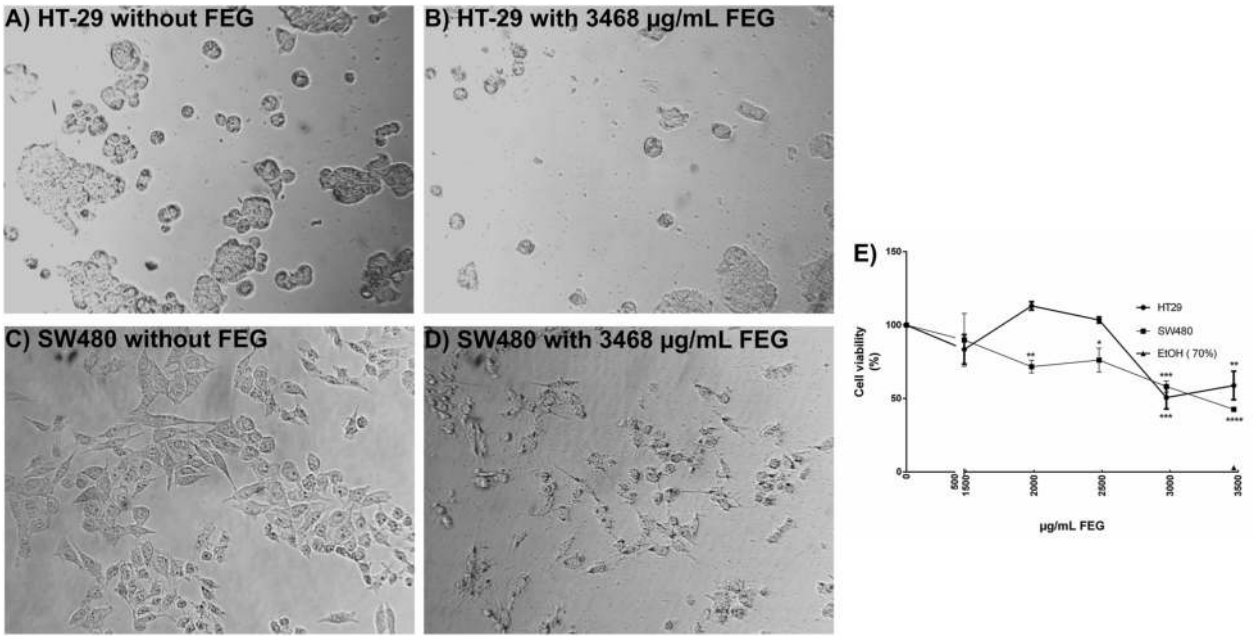

*Fig. 1. Fermented extract of garambullo (FEG) decreases cell viability in HT-29 and SW480 colorectal cancer cell lines. Representative micrographs showing the morphology of HT-29 and SW480 cells after 24 h of treatment. (A, C) HT-29 and SW480 cells without FEG (untreated cells). (B, D) Cells treated with 3468 μg/mL FEG. FEG exposure markedly reduced cell density and altered the elongated morphology characteristic of SW480 cells, resulting in a rounded, detached appearance. (E) Cell viability was evaluated by MTT assay after 24 h of treatment with FEG at concentrations of 0 (untreated control), 1487, 1982, 2478, 2973, and 3468 μg/mL. IC50 values of 2985 μg/mL for HT-29 and 3200 μg/mL for SW480 were used as reference concentrations. Ethanol (70%) was used as a positive control (0% viability). Data are expressed as mean ± SD from three independent experiments performed in triplicate. Statistical analysis was conducted separately for each cell line using one-way ANOVA followed by Dunnett's multiple comparisons test versus untreated control (*p < 0.05, **p < 0.01, ***p < 0.001,****p < 0.0001). MTT: thiazolyl blue tetrazolium bromide.*

月日知識庫

3468 μg/mL and 2973 μg/mL FEG reduced viability to 57% and 42%, respectively, after 24 h (Fig. 1E). Overall, both CRC cell lines displayed comparable IC_{50} values in response to FEG exposure.

3.2. FEG induces late apoptosis and necrosis in HT-29 and SW480 CRC cell lines

To evaluate the type of cell death induced by FEG in HT-29 and SW480 CRC cell lines, flow cytometry was performed post-treatment. The IC_{50} values previously determined by MTT assay were used: 2985 μg/mL for HT-29 and 3200 μg/mL for SW480 cells. To determine whether the observed cell death represented an acute cytotoxic event or a progressive process, a time-course analysis was performed. At the early time point (4 h post-treatment), no significant changes were observed in the distribution of live, apoptotic, or necrotic populations in either HT-29 or SW480 cells compared to untreated controls (Supplementary Fig. S1). In contrast, after 24 h of exposure to FEG, both cell lines exhibited a marked increase in cell death, as reflected by the shift in cell populations in the representative flow cytometry dot plots (Fig. 2A). HT-29 cells exhibited a statistically significant reduction in the percentage of live cells, showing a 59% decrease in FEG-treated cells compared to the control group ($p < 0.0001$) (Fig. 2B). This reduction was mainly due to late apoptosis (35%, $p < 0.0001$) and necrosis (23%, $p < 0.05$). No significant difference was observed in early apoptosis between treated and untreated HT-29 cells (Fig. 2B). In contrast, SW480 cells showed a 36% decrease in live cells following FEG treatment compared to untreated cells ($p < 0.0001$) (Fig. 2B). Although early apoptosis (11%) and late apoptosis (7%) were observed, these changes were not statistically significant. However, a significant increase in necrosis (20%) was detected in FEG-treated SW480 cells ($p < 0.05$) (Fig. 2B). These results indicate that FEG induces cell death in both CRC cell lines. In HT-29 cells, late apoptosis and necrosis were the predominant mechanisms, whereas in SW480 cells, necrosis was the main pathway induced, with early and late apoptosis remaining largely unchanged. These temporal differences suggest that the cell death induced by FEG is time-dependent and that the extensive necrosis detected at 24 h may, in part, represent secondary necrosis following an apoptotic cascade.

3.3. Inhibitory effect of FEG on colony formation in HT-29 and SW480 CRC cell lines

To evaluate the anti-clonogenic potential of FEG, three-dimensional (3D) colony formation assays were performed using increasing concentrations of FEG (37, 74, and 149 μg/mL). Visible colony growth was observed from day 7 onward. After 14 days, well-formed colonies were present in untreated HT-29 (Fig. 3A and B) and SW480 cells (Fig. 3C and D), confirming their clonogenic capacity. In HT-29 cells, no colonies were detected at any of the tested FEG concentrations (37, 74, and 149 μg/mL) (Fig. 4B–D) compared to untreated cells (Fig. 4A). Quantitative analysis confirmed a highly significant reduction at all concentrations ($p < 0.0001$) (Fig. 5F). Comparable anti-clonogenic effects were observed in SW480 cells. Representative images show a clear reduction in colony formation in FEG-treated groups (Fig. 5B–D) compared to the untreated cells (Fig. 5A). Quantitative analysis confirmed a significant decrease in colony numbers at 37 μg/mL ($p < 0.001$), 74 μg/mL ($p < 0.01$), and 149 μg/mL ($p < 0.0001$) (Fig. 5E), with complete suppression observed at the highest concentration. FEG significantly reduced colony formation in SW480 cells, while no colonies were observed in HT-29 cells at any tested concentration. These findings demonstrate, for the first time, the anti-clonogenic potential of FEG in both HT-29 and SW480 CRC cell lines.

3.4. In silico *molecular docking analysis of butyric acid with apoptosis- and necroptosis-related targets*

Molecular docking analyses were performed using SwissDock [28], which integrates the Attracting Cavities 2.0 algorithm [29], to evaluate the interaction of butyric acid with apoptosis- and necroptosis-related targets. To explore a potential mechanistic basis for the programmed cell death observed *in vitro*, molecular docking analyses were performed using butyric acid, a SCFA previously reported in FEG [15]. Docking simulations against Caspase-3 (PDB: 3DEI) generated eight clusters of possible binding conformations. Among these, Cluster 0 exhibited the most favorable binding energy ($\Delta G = -5.41$ kcal/mol; FullFitness = −39.41 kcal/mol) and was selected for detailed interaction analysis (Fig. 6A). The docking simulation positioned butyric acid within the catalytic region, suggesting possible structural compatibility. To further investigate the potential involvement of regulated necrosis pathways, docking analysis was also performed against RIPK1 (PDB: 4I5C). Cluster 0 displayed the most favorable interaction ($\Delta G = -5.18$ kcal/mol; FullFitness = −35.62 kcal/mol), indicating a theoretical binding compatibility between butyric acid and the RIPK1 kinase domain (Fig. 6B). Although predictive in nature, these *in silico* findings support a possible molecular interaction between FEG-

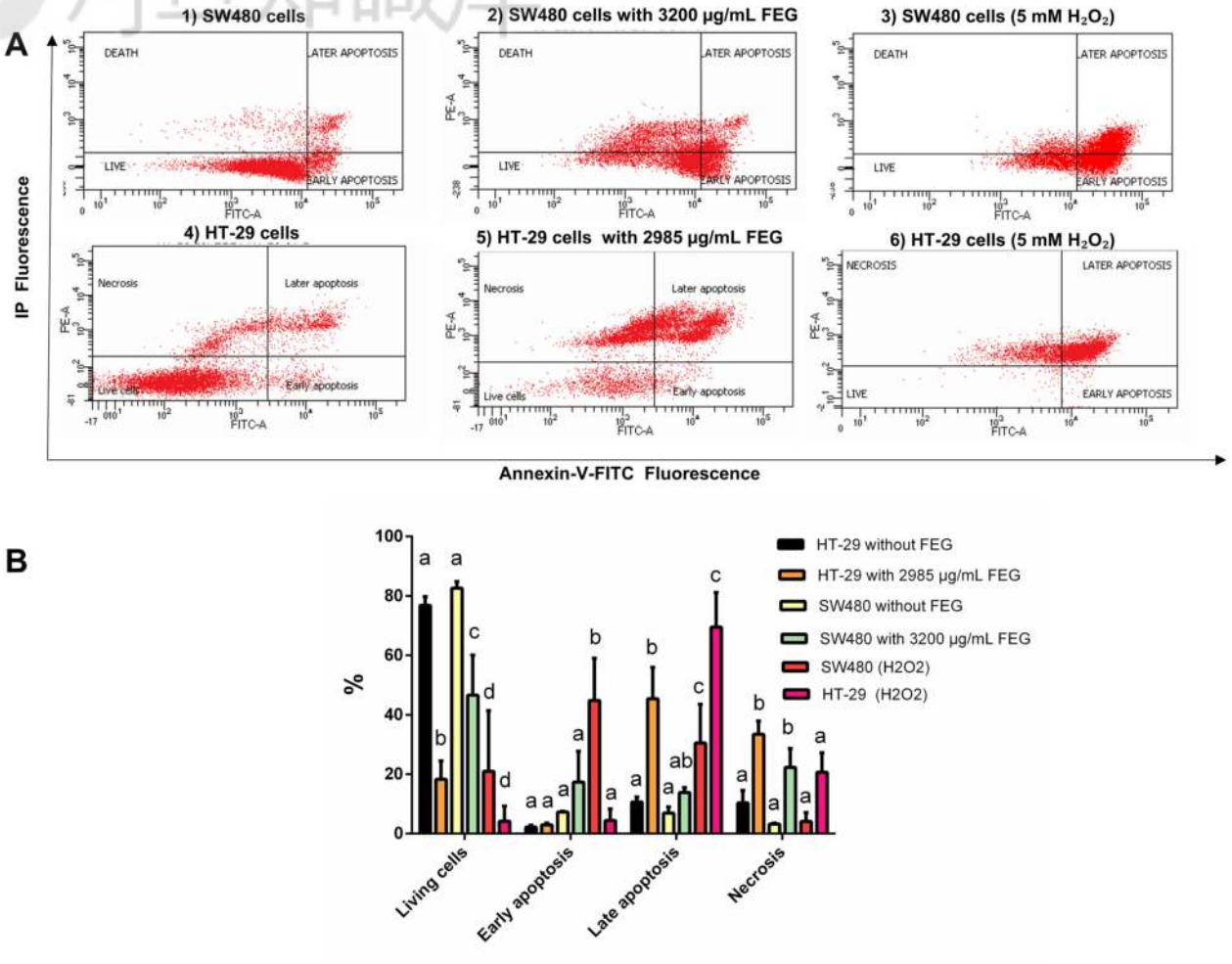

Fig. 2. FEG induces apoptosis and necrosis in HT-29 and SW480 colorectal cancer cell lines. (A) Representative dot plots of SW480 cells: untreated (A1), treated with 3200 µg/mL FEG (A2), or 5 mM H_2O_2 (positive control) (A3); and HT-29 cells: untreated (A4), treated with 2985 µg/mL FEG (A5), or 5 mM H_2O_2 (positive control) (A6). (B) Quantification of cell death showing mean percentages of live, early apoptotic, late apoptotic, and necrotic cells in untreated and FEG-treated HT-29 and SW480 cells after 24 h of exposure, alongside positive controls. Cells were stained with Annexin V and propidium iodide (PI) and analyzed by flow cytometry. Data are presented as mean ± SD from three independent experiments. Statistical analysis was performed using two-way ANOVA followed by Tukey's multiple comparisons test. Different letters above the bars indicate statistically significant differences ($p < 0.05$); groups sharing the same letter did not differ significantly. FEG: fermented extract of garambullo.

derived metabolites and key regulators of apoptosis and necroptosis, providing preliminary mechanistic context for the cytotoxic effects observed in HT-29 and SW480 cells.

4. Discussion

This work aimed to explore the potential anticancer effects of FEG, focusing on viability, apoptosis, and colony formation in HT-29 and SW480 CRC cell lines. Both cell lines exhibited a similar IC_{50} (2985 µg/mL and 3200 µg/mL), confirming that FEG, obtained through *in vitro* digestion and fermentation, reduces cell viability, induces apoptosis and necrosis, and exerts an anticlonogenic effect. The observed reduction in cell viability in HT-29 and SW480 cells may be attributed to the natural bioactive compounds present in garambullo, such as flavonols, hydroxycinnamic acids, hydroxybenzoic acids, betaxanthins, flavonoids, betalains, and ascorbic acid, among others [4,30]. In this context, Sánchez-Recillas et al. recently described, via metabolomic enrichment analysis, the relative abundance of major metabolites produced during various stages of *in vitro* colonic fermentation of garambullo (FE), specifically from its non-digestible fraction (NDF). Among the SCFAs detected, butyric acid showed a significant increase in the FE-NDF across the fermentation time points (6 and 24 h), reaching its maximum concentration at the end of the process [15]. Regarding garambullo, a berry that represents

月日知識庫

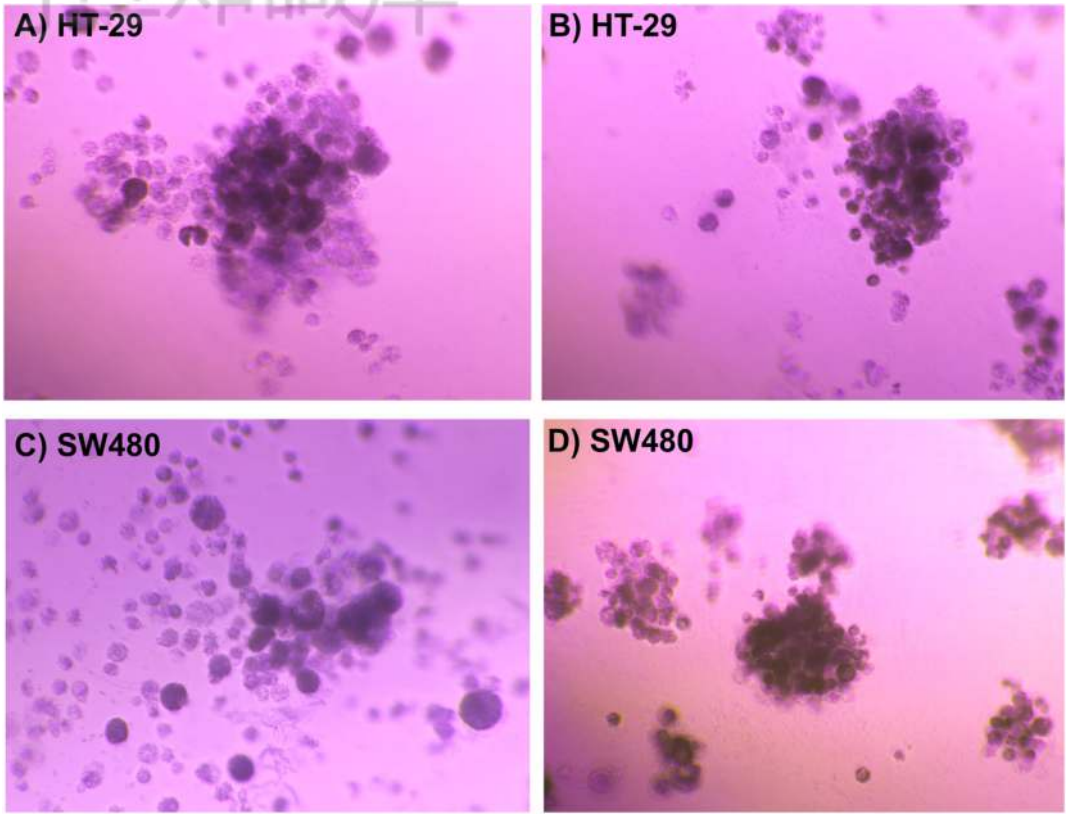

Fig. 3. Baseline 3D colony formation in HT-29 and SW480 colorectal cancer cell lines. Three-dimensional colony formation assays were performed using a bottom layer of 0.6% agarose, a middle layer of 0.3% agarose containing 5×10^4 HT-29 (A, B) or SW480 (C, D) cells, and a top liquid layer of DMEM without FEG. After 14 days of incubation, colonies were stained with 0.5 mg/mL NBT and incubated overnight. Representative images were captured at 25X magnification using a Luzeren microscope equipped with Velab software. Viable colonies are visualized as dark blue to purple-stained clusters. FEG, fermented extract of garambullo; NBT, nitrotetrazolium blue chloride; PBS, phosphate-buffered saline.

a relatively new area of research, previous studies have demonstrated that its phytochemicals can modulate cancer cell behavior through various biological processes, including proliferation, migration, and apoptosis [22,23]. Phenolic compounds, for example, have demonstrated cytotoxic activity against cancer cell lines, such as breast cancer (MCF-7), human prostate cancer (PC-3), and lung cancer (A549) cells [31]. Additionally, other compounds found in garambullo, such as peniocerol and macdougallin, have been reported to inhibit cell proliferation, induce cell cycle arrest, and promote apoptosis in colon cancer cell lines, including SW620, HCT-15, and HCT-116 [22,23]. Given these findings, a key aim of the present study was to determine whether the observed reduction in cell viability by FEG was associated with the induction of apoptosis. Apoptosis is a tightly regulated process that eliminates damaged or unnecessary cells through a cascade of molecular events involving the activation of cysteine proteases known as caspases. These are typically classified as initiator caspases (e.g., 2, 8, 9, and 10) and executioner caspases (e.g., 3 and 7). In cancer cells, resistance to apoptosis is a hallmark feature, often resulting from altered expression of pro-apoptotic or anti-apoptotic genes [16]. Among the most relevant findings, we observed that HT-29 cells exhibited increased levels of late apoptosis and necrosis, while SW480 cells showed a pronounced increase in necrosis upon treatment with FEG, compared to untreated cells. This differential apoptotic response may be associated with the specific carcinogenesis stage represented by each cell line. Although both are derived from human colorectal adenocarcinoma, HT-29 is classified as Duke's Stage B, whereas SW480 cells correspond to a more advanced Duke-type B/C stage, according to ATCC technical specifications. These inherent phenotypic differences likely influence their distinct sensitivities and the activation of different cell death pathways in response to FEG. These observations are further supported by unpublished data from our research group, where protein array analysis revealed that FEG treatment modulates the expression of necroptosis-related proteins in

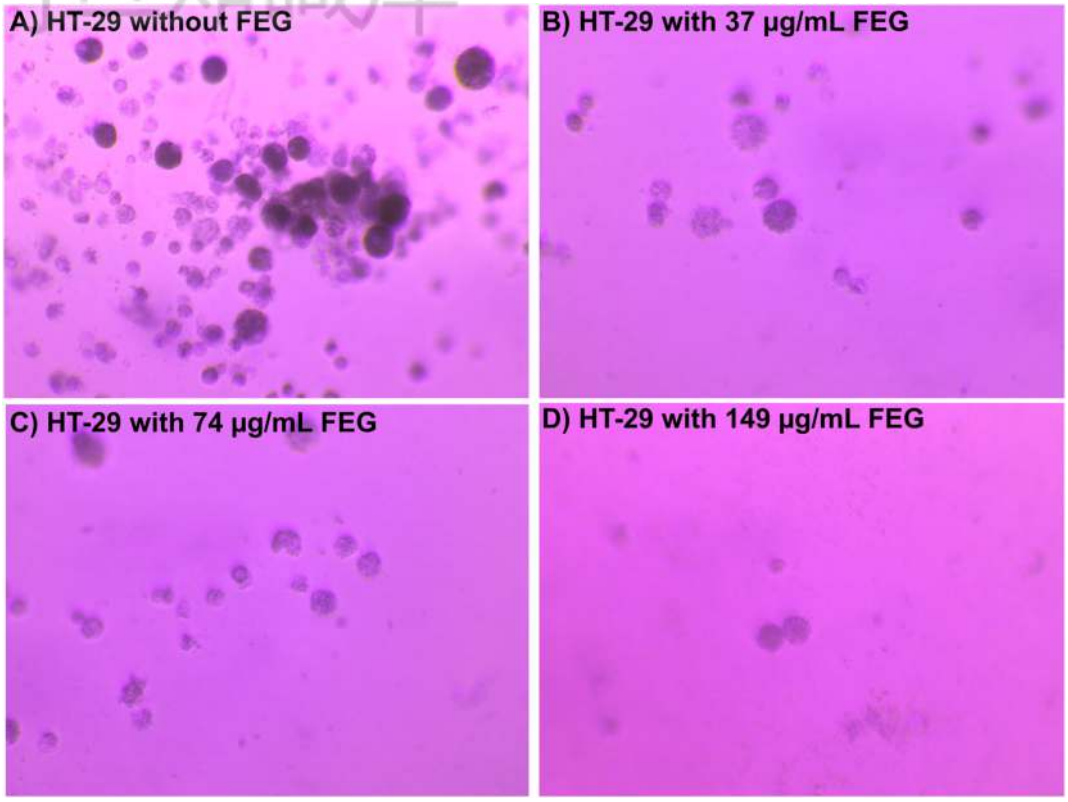

Fig. 4. Representative effect of FEG on 3D colony formation in the HT-29 cell line. Three-dimensional colony formation assays were conducted using a bottom layer of 0.6% agarose, a middle layer of 0.3% agarose containing 5×10^4 HT-29 cells, and a top liquid layer of DMEM either without FEG (A) or supplemented with 37 μg/mL FEG (B), 74 μg/mL FEG (C), or 149 μg/mL FEG (D). After 14 days of incubation, colonies were stained with 0.5 mg/mL NBT and incubated overnight. Representative images were captured at 25X magnification using a Luzeren microscope equipped with Velab software. Viable colonies are visualized as dark blue to purple-stained clusters. FEG, fermented extract of garambullo; NBT, nitrotetrazolium blue chloride; PBS, phosphate-buffered saline.

SW480 cells. Other natural extracts have also demonstrated cytotoxic effects on CRC cells; notably, an aqueous extract of freeze-dried mango pulp (LMPE), rich in bioactive compounds, exhibited cytotoxic activity against SW480 cells and their metastatic derivative SW620 by inducing oxidative stress, cell cycle arrest, and apoptosis [32]. Similarly, Gutiérrez-Silerio et al. [33] reported that a methanolic extract of Hass avocado mesocarp induced cytotoxicity and apoptosis in HT-29 cells after 48 h of treatment. Furthermore, strawberry tree honey (STH), a polyphenol-enriched natural product, enhanced the efficacy of 5-fluorouracil (5-FU) by reducing cell viability and upregulating key apoptotic markers such as p53, cleaved PARP (c-PARP), and caspase-3 in HCT-116 and LoVo CRC cells [34]. In addition, black tea extracts containing flavanol-3-ols, theaflavins, and thearubigins have shown anti-oncogenic effects through synergistic actions that promote apoptosis and cell cycle arrest in HCT-116 colon cancer cells [35]. Beyond apoptosis, necrosis can also occur in a regulated and programmed manner, a process known as necroptosis. This concept was formally introduced by Yuan and colleagues in 2005 following the identification of Necrostatin-1 (Nec-1), a small-molecule inhibitor of receptor-interacting protein kinase 1 (RIPK1), which demonstrated that necrotic cell death could be genetically and pharmacologically controlled [36,37]. When apoptosis is inhibited, tumor necrosis factor (TNF) can trigger necroptotic cell death in certain cell types. The key mediators of necroptosis include receptor-interacting protein kinase 1 (RIPK1), RIPK3, and mixed lineage kinase domain-like protein (MLKL), which are all inhibited by Nec-1. Necroptosis is characterized by features resembling necrosis, including plasma membrane rupture, cytoplasmic translucency, and organelle swelling [36,38]. In this context, shikonin, a natural naphthoquinone compound derived from the roots of Lithospermum erythrorhizon (Zicao), was the first phytochemical identified to induce necroptosis in osteosarcoma, glioma, hematopoietic, and multiple myeloma cell lines [37]. Although direct transcriptomic or proteomic validation was not performed in the present

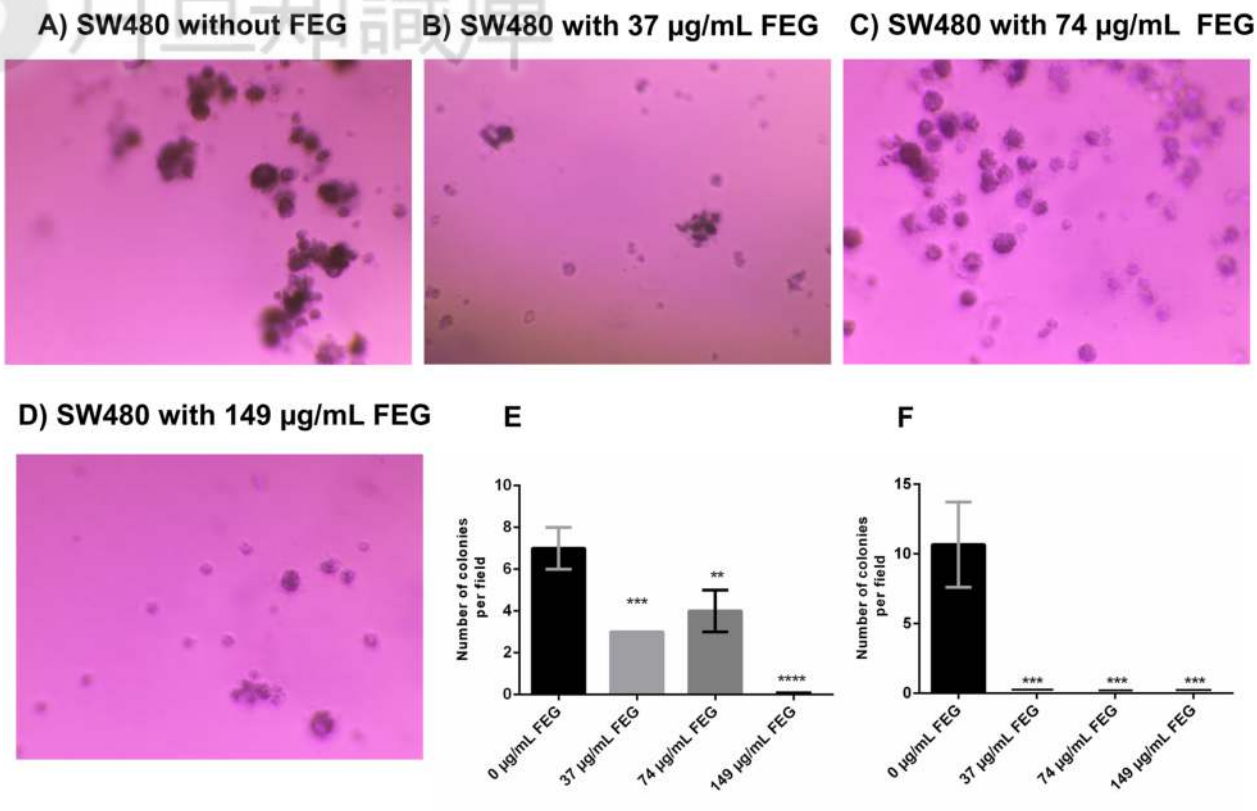

*Fig. 5. Inhibitory effect of FEG on colony formation in colorectal cancer cell lines. Three-dimensional assays were performed using SW480 cells with a bottom layer of 0.6% agarose, a middle layer of 0.3% agarose containing 5 × 104 cells, and a top liquid layer of DMEM either without FEG (A) or supplemented with 37 µg/mL FEG (B), 74 µg/mL FEG (C), or 149 µg/mL FEG (D). After 14 days, colonies were stained with 0.5 mg/mL NBT and imaged at 25X magnification. Viable colonies appear as dark blue to purple clusters. Quantification of colony formation in SW480 (E) and HT-29 (F) cells is shown. Quantitative analysis demonstrates significant inhibition of colony formation in SW480 cells and complete absence of colonies in HT-29 cells across the tested concentrations. Data are presented as mean ± SD of the average number of colonies quantified from three independent microscopic fields per condition (n = 3). Statistical analysis was performed independently for each cell line using ordinary one-way ANOVA followed by Dunnett's multiple comparisons test. Levels of significance are indicated in the figure as follows: *p < 0.05, **p < 0.01, ***p < 0.001, and ****p < 0.0001. FEG, fermented extract of garambullo; NBT, nitrotetrazolium blue chloride; PBS, phosphate-buffered saline.*

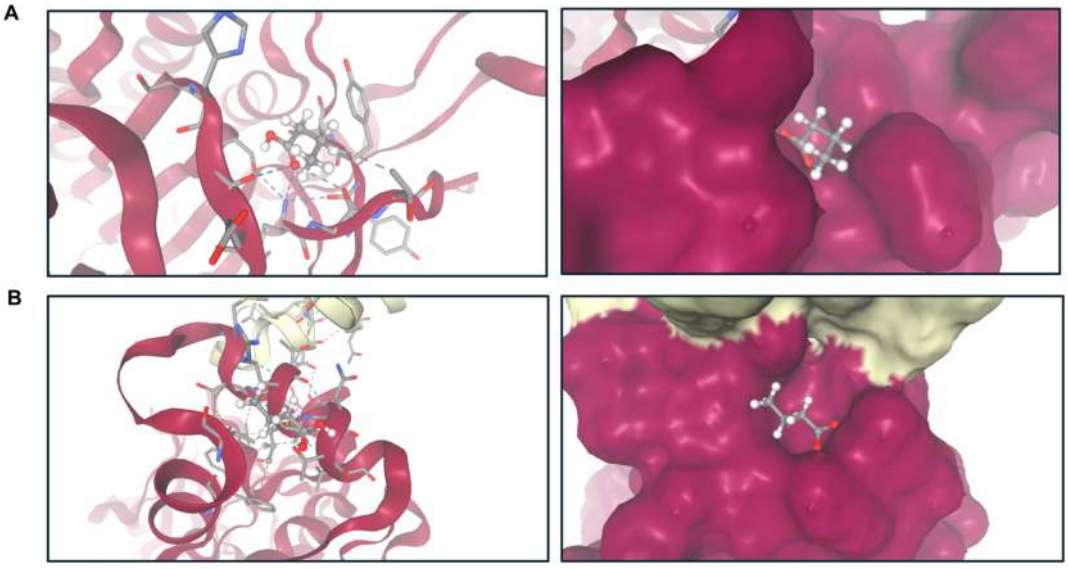

Fig. 6. Molecular docking analysis of butyric acid with apoptosis- and necroptosis-related targets.(A) Predicted binding pose within the catalytic site of human Caspase-3 (PDB: 3DEI), showing a binding energy (ΔG) of −5.41 kcal/mol and a FullFitness score of −39.41 kcal/mol. (B) Interaction with the RIPK1 kinase domain (PDB: 4I5C), exhibiting a ΔG of −5.18 kcal/mol and a FullFitness of −35.62 kcal/mol. For each panel, the left image shows the ribbon representation with specific intermolecular interactions (blue dashed lines indicate hydrogen bonds; dotted gray lines represent hydrophobic contacts). The right image shows the solvent-accessible surface, illustrating the predicted insertion of butyric acid into the binding pocket (highlighted in magenta).

月日知識庫

study, previous metabolomic characterization of fermented garambullo identified bioactive SCFAs, such as butyric acid. These metabolites are recognized modulators of CRC cell fate, exerting anti-proliferative and pro-apoptotic effects and inhibiting colony formation in experimental models [39]. In this regard, we performed complementary *in silico* docking analyses to provide a preliminary mechanistic rationale for these findings. Our results suggest that butyric acid shows potential for molecular interaction with key regulators of cell death, including Caspase-3 and RIPK1. Although predictive in nature, these findings offer a plausible molecular context consistent with the apoptotic and necrosis-associated responses observed in HT-29 and SW480 cells, respectively. Future studies incorporating pathway-specific inhibitors (e.g., Nec-1), gene expression analyses, or protein-level validation will be necessary to determine the precise signaling mechanisms involved.

Following the characterization of the cell death mechanisms and the potential molecular interactions identified through docking, an additional significant contribution to evaluating the anti-clonogenic potential of FEG was achieved through 3D agarose-based assays. These assays are characterized by the anchorage-independent growth of cancer cells, which do not adhere to the culture plate surface [24]. To the best of our knowledge, this study represents the initial evaluation of a natural extract, specifically FEG, on colorectal cancer cell lines using a 3D agarose-based culture model. After 14 days without FEG treatment in the 3D assays, well-formed colonies were observed in both HT-29 and SW480 CRC cell lines. However, exposure to only 149 μg/mL FEG resulted in a complete inhibition of colony formation in both lines, indicating a potent anti-clonogenic effect of FEG in a three-dimensional environment at low concentrations. Notably, HT-29 cells exhibited greater sensitivity to FEG compared to SW480 cells. This observation underscores the importance of using 3D systems, as a major advantage of this assay is that only tumorigenic cells can form colonies in agarose, thereby allowing for a semi-quantitative evaluation of different treatments [24,25], such as antioxidants or natural extracts like FEG, at varying concentrations. It is noteworthy that 3D cultures generally respond to lower concentrations of natural compounds compared with 2D models. For example, agar-derived sugars from red seaweeds inhibited HCT-116 human colon cancer cells colony formation at 10–100 μg/mL [40], which is consistent with the effective range of FEG observed in our 3D assays (37–149 μg/mL). Current 3D assays in cancer research provide more physiologically relevant data regarding cell–cell interactions, tumor characteristics, drug development, metabolic profiling, stem cell research, and other disease models [41]. Our findings demonstrate a clear anti-clonogenic effect of FEG on HT-29 and SW480 cells, suggesting the value of extending these studies to other CRC cell lines. CRC ranked among the top ten most common cancers worldwide in 2020 for both men and women [19]. In this context, the implementation of *in vitro* gastrointestinal digestion and fermentation models enabled the evaluation of FEG under physiologically relevant conditions, providing additional translational relevance to our findings in colorectal cancer models.

In summary, this study demonstrates that the Mexican endemic fruit garambullo (*M. geometrizans*) exhibits anti-proliferative and pro-apoptotic effects in 2D assays, as well as marked inhibition of colony formation in 3D models. Late apoptosis was identified as the predominant mechanism of cell death, followed by necrosis, in both HT-29 and SW480 cell lines. Complementary *in silico* docking analyses suggest that butyric acid, a previously identified component of FEG, may interact with key regulators of cell death, including Caspase-3 and RIPK1, providing a plausible mechanistic framework consistent with the observed *in vitro* effects. Moreover, the use of a physiologically relevant gastrointestinal digestion and fermentation model strengthens the translational relevance of FEG under conditions that mimic human digestion, highlighting this endemic fruit as a promising candidate for further preclinical investigation and a natural resource worthy of conservation.

Funding statement

This research study was supported by SECIHTI-Ciencia de Frontera (Grant no.1560335).

Conflicts of interest

The authors declare no conflict of interest.

Acknowledgements

The authors gratefully acknowledge the School of Chemistry at Universidad Autónoma de Querétaro (Campos-Vega's Lab) for providing the facilities necessary to carry out the garambullo fermentation. We also thank Dr. Feller's laboratory at the Charles Tanford Protein Centre in Halle, Germany, for the training provided in the 3D cell culture technique.

Guadalupe Soledad López-Álvarez acknowledges the support of SECIHTI through the postdoctoral fellowship program: Estancias Posdoctorales por México 2022-1.

月旦知識庫

Appendix

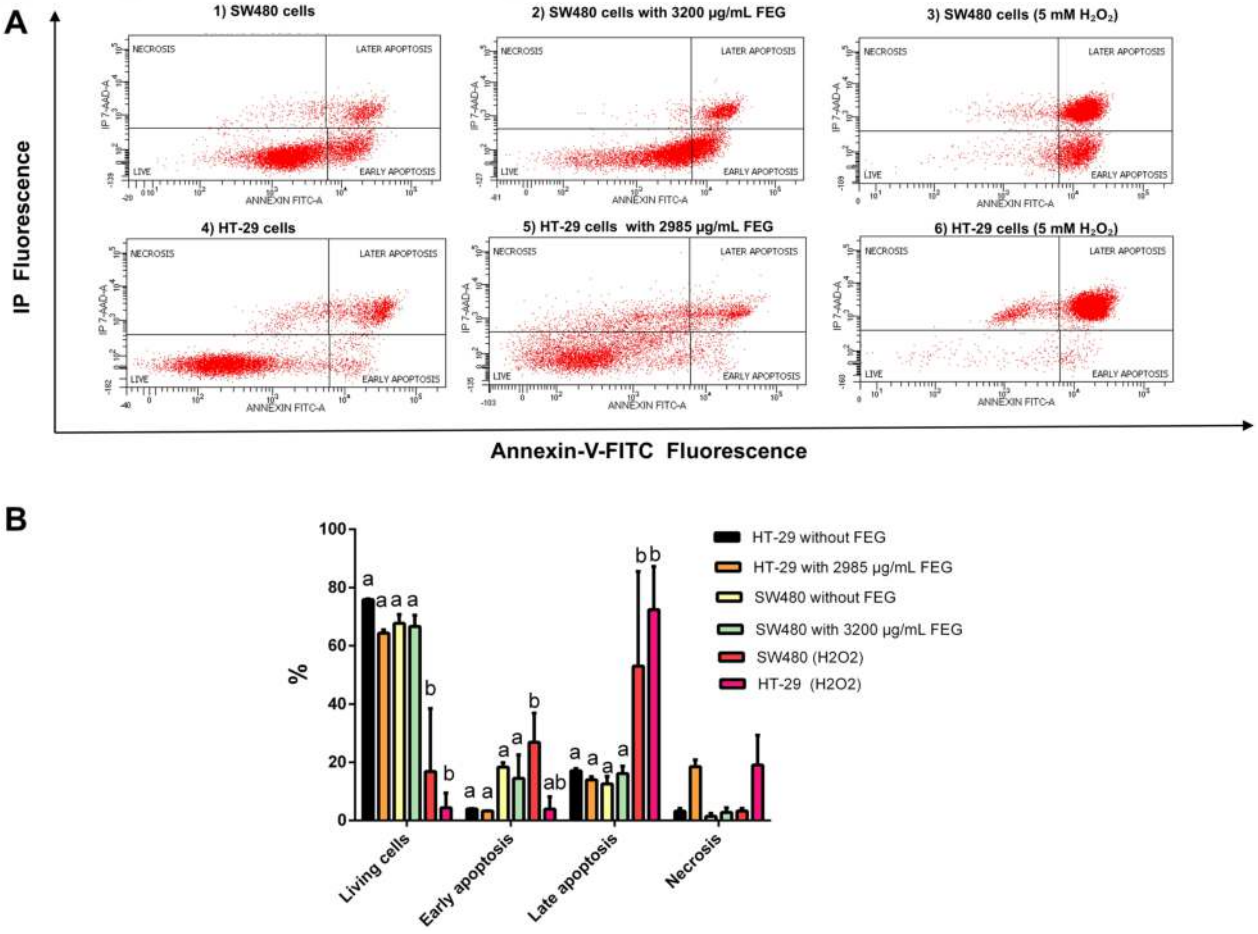

Fig. S1. Early effects of FEG on apoptosis and necrosis at 4 h post-treatment in HT-29 and SW480 colorectal cancer cell lines. (A) Representative flow cytometry dot plots of SW480 cells: untreated (A1), treated with 3200 µg/mL FEG (A2), or 5 mM H_2O_2 (positive control) (A3); and HT-29 cells: untreated (A4), treated with 2985 µg/mL FEG (A5), or 5 mM H_2O_2 (positive control) (A6). (B) Quantification of cell death showing the mean percentages of live, early apoptotic, late apoptotic, and necrotic cells in untreated and FEG-treated HT-29 and SW480 cells after 4 h of exposure, including positive controls. Cells were stained with Annexin V and propidium iodide (PI) and analyzed by flow cytometry. Data are presented as mean ± SD from three independent experiments. Different letters above the bars indicate statistically significant differences according to Tukey's multiple comparisons test ($p < 0.05$); groups sharing the same letter do not differ significantly. FEG, fermented extract of garambullo.

References

[1] Guzmán-Maldonado SH, Herrera-Hernández G, Hernández-López D, Reynoso-Camacho R, Guzmán-Tovar A, Vaillant F, et al. Physicochemical, nutritional and functional characteristics of two underutilised fruit cactus species (Myrtillocactus) produced in central Mexico. Food Chem 2010;121(2).

[2] Montiel-Sánchez M, García-Cayuela T, Gómez-Maqueo A, García HS, Cano MP. In vitro gastrointestinal stability, bioaccessibility and potential biological activities of betalains and phenolic compounds in cactus berry fruits (Myrtillocactus geometrizans). Food Chem 2021;342.

[3] Sandoval-Salazar C, Jiménez-García SN, Beltrán-Campos V, Vera-Becerra LE, Núñez-Colín CA. Effect of berrycactus fruit (Myrtillocactus geometrizans) on glutamate, glutamine, and GABA levels in the frontal cortex of rats fed with a high-fat diet. Open Life Sci 2023;18(1).

[4] Sánchez-Recillas E, Campos-Vega R, Pérez-Ramírez IF, Luzardo-Ocampo I, Cuéllar-Núñez ML, Vergara-Castañeda HA. Garambullo (Myrtillocactus geometrizans): effect of in vitro gastrointestinal digestion on the bioaccessibility and antioxidant capacity of phytochemicals. Food Funct 2022;13.

[5] Bouyahya A, El Omari N, El Hachlafi N, El Jemly M, Hakkour M, Balahbib A, et al. Chemical compounds of berry-derived polyphenols and their effects on gut microbiota, inflammation, and cancer. Molecules 2022;27.

[6] Ruíz-Aguilar I, Meza-Márquez OG, Osorio-Revilla G, Gallardo-Velázquez T, Ramos-Monroy OA. Phytochemical compounds, and antioxidant, anti-hyperglycemic, and anti-inflammatory activity of microencapsulated Garambullo (Myrtillocactus geometrizans) extract during in vitro digestion and storage. Processes 2024 Nov 1;12(11).

[7] Agudelo CD, Luzardo-Ocampo I, Campos-Vega R, Loarca-Pina G, Maldonado-Celis ME. Bioaccessibility during in vitro digestion and antiproliferative effect of bioactive compounds from Andean Berry (Vaccinium meridionale Swartz) juice. J Agric Food Chem 2018;66(28).

[8] McDougall GJ, Ross HA, Ikeji M, Stewart D. Berry extracts exert different antiproliferative effects against cervical and colon cancer cells grown in vitro. J Agric Food Chem 2008;56(9).

月日知識庫

[9] Zhao C, Giusti MM, Malik M, Moyer MP, Magnuson BA. Effects of commercial anthocyanin-rich on colonic cancer and nontumorigenic colonic cell growth. J Agric Food Chem 2004;52(20).

[10] Lala G, Malik M, Zhao C, He J, Kwon Y, Giusti MM, et al. Anthocyanin-rich extracts inhibit multiple biomarkers of colon cancer in rats. In: Nutrition and cancer; 2006.

[11] Al-Ishaq RK, Overy AJ, Büsselberg D. Phytochemicals and gastrointestinal cancer: cellular mechanisms and effects to change cancer progression. Biomolecules 2020;10.

[12] Altemimi A, Lakhssassi N, Baharlouei A, Watson DG, Lightfoot DA. Phytochemicals: extraction, isolation, and identification of bioactive compounds from plant extracts. Plants 2017;6.

[13] Ionescu VA, Diaconu CC, Gheorghe G, Mihai MM, Diaconu CC, Bostan M, et al. Gut microbiota and colorectal cancer: a balance between risk and protection. International journal of molecular sciences, vol. 26. Multidisciplinary Digital Publishing Institute (MDPI); 2025.

[14] De Filippo C, Chioccioli S, Meriggi N, Troise AD, Vitali F, Mejia Monroy M, et al. Gut microbiota drives colon cancer risk associated with diet: a comparative analysis of meat-based and pesco-vegetarian diets. Microbiome 2024 Dec 1; 12(1):180.

[15] Sánchez-Recillas E, Almanza-Aguilera E, Dufoo-Hurtado E, Luzardo-Ocampo I, Campos-Vega R, Vergara-Castañeda HA. Untargeted metabolomics of gut-derived metabolites from in vitro colonic fermentation of garambullo (Myrtillocactus geometrizans). J Funct Foods 2024;114.

[16] Fernald K, Kurokawa M. Evading apoptosis in cancer. Trends Cell Biol 2013;23.

[17] Hanahan D. Hallmarks of cancer: new dimensions. Cancer Discov 2022;12.

[18] Ionescu VA, Gheorghe G, Bacalbasa N, Chiotoroiu AL, Diaconu C. Colorectal cancer: from risk factors to oncogenesis, vol. 59. Medicina (Lithuania); 2023.

[19] Sung H, Ferlay J, Siegel RL, Laversanne M, Soerjomataram I, Jemal A, et al. Global cancer statistics 2020: GLOBOCAN estimates of incidence and mortality worldwide for 36 cancers in 185 countries. CA Cancer J Clin 2021;71(3).

[20] Ferlay J, Colombet M, Soerjomataram I, Parkin DM, Piñeros M, Znaor A, et al. Cancer statistics for the year 2020: an overview. Int J Cancer 2021;149(4).

[21] Godínez-Santillán RI, Kuri-García A, Ramírez-Pérez IF, Herrera-Hernández MG, Ahumada-Solórzano SM, Guzmán-Maldonado SH, et al. Characterization of extractable and non-extractable phenols and betalains in berry-cactus (Myrtillocactus geometrizans) and its chemoprotective effect in early stage of Colon cancer in vivo. Antioxidants 2024 Sep 1;13(9).

[22] Couder-García B del C, Jacobo-Herrera NJ, Zentella-Dehesa A, Rocha-Zavaleta L, Tavarez-Santamaría Z, Martínez-Vázquez M. The phytosterol peniocerol inhibits cell proliferation and tumor growth in a Colon cancer xenograft model. Front Oncol 2019;9.

[23] Bolaños-Carrillo MA, Ventura-Gallegos JL, Saldivar-Jiménez AD, Zentella-Dehesa A, Martínez-Vázquez M. Effect of sterols isolated from Myrtillocactus geometrizans on growth inhibition of Colon and breast cancer cells. Evid Based Complement Alternat Med 2015;2015.

[24] Borowicz S, Van Scoyk M, Avasarala S, Karuppusamy Rathinam MK, Tauler J, Bikkavilli RK, et al. The soft agar colony formation assay. JoVE J 2014;(92).

[25] Du F, Zhao X, Fan D. Soft Agar colony Formation assay as a hallmark of carcinogenesis. Bio Protoc 2017;7(12).

[26] Campos-Vega R, Vázquez-Sánchez K, López-Barrera D, Loarca-Piña G, Mendoza-Díaz S, Oomah BD. Simulated gastrointestinal digestion and in vitro colonic fermentation of spent coffee (Coffea arabica L.): bioaccessibility and intestinal permeability. Food Res Int 2015;77.

[27] Stein K, Borowicki A, Scharlau D, Scheu K, Brenner-Weiß G, Obst U, et al. Modification of an in vitro model simulating the whole digestive process to investigate cellular endpoints of chemoprevention. Br J Nutr 2011;105(5).

[28] Bugnon M, Röhrig UF, Goullieux M, Perez MAS, Daina A, Michielin O, et al. SwissDock 2024: major enhancements for small-molecule docking with Attracting Cavities and AutoDock Vina. Nucleic Acids Res 2024;52(W1).

[29] Röhrig UF, Goullieux M, Bugnon M, Zoete V. Attracting cavities 2.0: improving the flexibility and robustness for small-molecule docking. J Chem Inf Model 2023;63(12).

[30] Martínez EMM, Sandate-Flores L, Rodríguez-Rodríguez J, Rostro-Alanis M, Parra-Arroyo L, Antunes-Ricardo M, et al. Underutilized mexican plants: screening of antioxidant and antiproliferative properties of mexican cactus fruit juices. Plants 2021;10(2).

[31] Guía-García JL, Charles-Rodríguez AV, López-Romero JC, Torres-Moreno H, Genisheva Z, Robledo-Olivo A, et al. Phenolic composition and biological properties of rhus microphylla and myrtillocactus geometrizans fruit extracts. Plants 2021;10(10).

[32] Lozano-Casabianca GA, Arango-Varela SS, Aguillón-Osma J, Llano-Ramírez MA, Maldonado-Celis ME. Inhibition of cell proliferation and induction of cell cycle arrest in Colon cancer cells by lyophilized mango (Mangifera indica L.) pulp extract. Prev Nutr Food Sci 2022;27(4).

[33] Gutierrez-Silerio GY, Garcia-Solis P, Yahia EM, Núñez-Ríos JD, Vázquez-Cuevas F, Rodriguez-Salinas PA, et al. Cytotoxic and antitumoral effects of methanolic extracts of avocado fruit mesocarp in colorectal cancer cell line HT29. J Med Food 2024;27(3).

[34] Afrin S, Giampieri F, Cianciosi D, Alvarez-Suarez JM, Bullon B, Amici A, et al. Strawberry tree honey in combination with 5-fluorouracil enhances chemosensitivity in human colon adenocarcinoma cells. Food Chem Toxicol 2021;156.

[35] Imran A, Butt MS, Xiao H, Imran M, Rauf A, Mubarak MS, et al. Inhibitory effect of black tea (Camellia sinensis) theaflavins and thearubigins against HCT 116 colon cancer cells and HT 460 lung cancer cells. J Food Biochem 2019;43(5).

[36] Liu ZG, Jiao D. Necroptosis, tumor necrosis and tumorigenesis. Cell Stress 2020;4(1).

[37] Yu J, Zhong B, Chen X. Induction of programmed necrosis by phytochemicals in colorectal cancer. In: Drug resistance in colorectal cancer: molecular mechanisms and therapeutic strategies; 2020.

[38] Gong Y, Fan Z, Luo G, Yang C, Huang Q, Fan K, et al. The role of necroptosis in cancer biology and therapy, vol. 18. Molecular Cancer; 2019.

[39] Gomes S, Baltazar F, Silva E, Preto A. Microbiota-Derived short-chain fatty acids: new road in colorectal cancer therapy. Pharmaceutics 2022;14(11).

[40] Yun EJ, Yu S, Kim YA, Liu JJ, Kang NJ, Jin YS, et al. In vitro prebiotic and anti-colon cancer activities of agar-derived sugars from red seaweeds. Mar Drugs 2021;19(4).

[41] Jensen C, Teng Y. Is it time to start transitioning from 2D to 3D cell culture? Front Mol Biosci 2020;7.